Electronic Supplementary Information

Electrochemiluminescence of Iridium(III)/Ruthenium(II) Complexes with Naphthyl Tags in Solutions and in Host-Guest Thin Films

Weiyu Qu,[†] Xinrui Yang,[†] Xiaojin Huang,[†] Weiliang Guo*,[†] and Zhihui Dai*,[†,‡]

[†]Collaborative Innovation Center of Biomedical Functional Materials and Key Laboratory of Biofunctional Materials of Jiangsu Province, School of Chemistry and Materials Science, Nanjing Normal University, Nanjing 210023, P. R. China

[‡]School of Chemistry and Molecular Engineering, Nanjing Tech University, Nanjing 211816, P. R. China

Corresponding Authors: Weiliang Guo, Email: guowl@njnu.edu.cn;
Zhihui Dai, Email: daizhihuii@njnu.edu.cn

Table of Contents

S1. Synthesis of ECL Luminophores

Coupling reaction was used for synthesizing the ancillary ligands, namely 4-(2-naphthalenyl)-1,10-phenanthroline (napphen), and 4-(2-naphthalenyl)-2,2′-bipyridine (napbpy). Nonoyama reaction was employed to obtain the bis μ-chloro dinuclear Ir(III) complex $(ppy)_2$-Ir-μ-Cl_2. Coordination reaction was used to yield cationic Ir(III)/Ru(II) complexes.[S1, S2] **Fig. 1** displays the molecular structures of Ir(III)/Ru(II) complexes, namely (1,10-phenanthroline)bis[2-(2-pyridinyl)phenyl]iridium(III) ($Ir(ppy)_2(phen)^+$, **1**), (1,10-phenanthroline)bis(2,2'-bipyridine)ruthenium(II) ($Ru(bpy)_2(phen)^{2+}$, **2**), tris(2,2'-bipyridine)ruthenium(II) ($Ru(bpy)_3^{2+}$, **3**) [4-(2-naphthalenyl)-1,10-phenanthroline]bis[2-(2-pyridinyl)phenyl]iridium(III) ($Ir(ppy)_2(napphen)^+$, **4**), [4-(2-naphthalenyl)-1,10-phenanthroline]bis(2,2'-bipyridine)ruthenium(II) ($Ru(bpy)_2(napphen)^{2+}$, **5**), and [4-(2-naphthalenyl)-2,2'-bipyridine]bis(2,2'-bipyridine)ruthenium(II) ($Ru(bpy)_2(napbpy)^{2+}$, **6**). Synthesis details of these compounds were described in **Figs. S1-S5**.

S1.1. Synthesis of N^N ligands

Ligand 4-(2-naphthalenyl)-1,10-phenanthroline (**napphen**) was prepared in the following procedure. 5-Bromo-1,10-phenanthroline (110 mg, 0.43 mmol), (2-naphthalenyl) boronic acid (147.0 mg, 0.85 mmol) and Na_2CO_3 (490 mg, 4.67 mmol) were dissolved in tetrahydrofuran (32 mL) and water (3.9 mL), and Pd $(PPh_3)_4$ (24.6 mg, 0.021 mmol) was then added. After being refluxed at 80 ℃ for 24 h, the organic layer was collected by performing extraction with dichloromethane (10 mL × 3), washed with water (15 mL) and saturated brine (15 mL), and dried by Na_2SO_4. After being purified by column chromatography and eluting with ethyl acetate: petroleum ether = 1: 3, the ligand was obtained as a white solid (89.8 mg, 68.2%). ^{1}H NMR (400 MHz, Chloroform-*d*) δ 9.26 (s, 2H), 8.33 (dd, *J* = 12.6, 8.3 Hz, 2H), 8.04 (d, *J* = 7.0 Hz, 2H), 8.01–7.94 (m, 2H), 7.88 (s, 1H), 7.74–7.65 (m, 2H), 7.61 (dd, *J* = 6.5, 3.2 Hz, 3H).

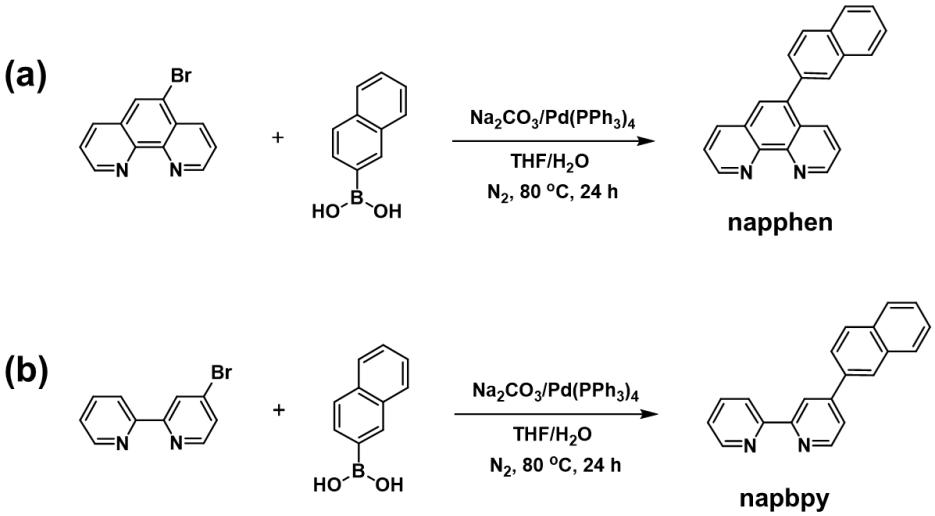

Fig. S1 Illustration of the synthesis of two ancillary ligands (N^N), namely (a) napphen and (b) napbpy.

Ligand 4-(2-naphthalenyl)-2,2′-bipyridine (**napbpy**) was prepared following same way expect that 5-bromo-1,10-phenanthroline was replaced by 4-bromo-2,2′-bipyridine. The product was obtained as a white solid (85.0 mg, 70.5%). ^{1}H NMR (400 MHz, Chloroform-*d*) δ 8.87 (s, 1H), 8.81 (d, *J* = 5.2 Hz, 1H), 8.78 (d, *J* = 4.6 Hz, 1H), 8.56 (d, *J* = 7.9 Hz, 1H), 8.31 (s, 1H), 8.00 (t, *J* = 8.3 Hz, 2H), 7.96–7.88 (m, 3H), 7.74 (d, *J* = 5.2 Hz, 1H), 7.61–7.53 (m, 2H), 7.40 (dd, *J* = 7.5, 4.8 Hz, 1H).

S1.2. Synthesis of bis *μ*-chloro dinuclear Ir(III) complex

The bis *m*-chloro dinuclear Ir(III) complex $(ppy)_2$-Ir-*m*-Cl_2 was synthesized according to the previous literature.[S3, S4]

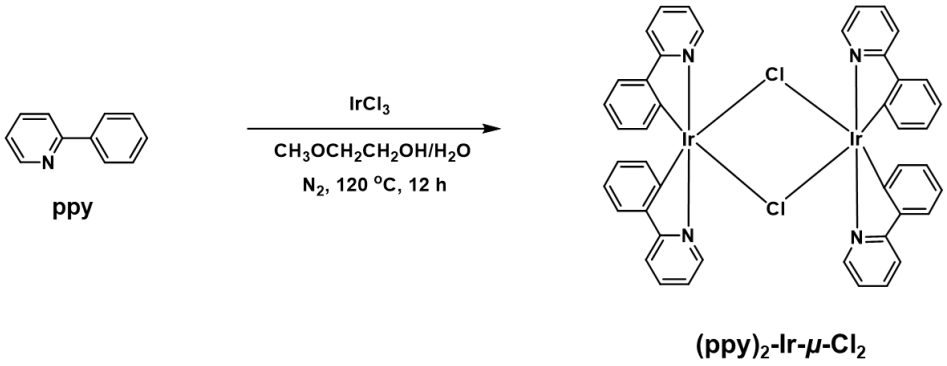

Fig. S2 Illustration of synthesis of bis μ-chloro dinuclear Ir(III) complex $(ppy)_2$-Ir-μ-Cl_2.

S1.3. Synthesis of Ir(III) complexes

$Ir(ppy)_2(phen)^+$ (1). Dissolved in dichloromethane (15 mL) and methanol (9 mL), the mixture of 1,10-phenanthroline (0.2 mmol, 36 mg) and $(ppy)_2$-Ir-μ-Cl_2 (0.1 mmol, 108.6 mg) was stirred at 55 °C for 16 h. Then the reactant was extracted by dichloromethane and water, washed with saturated brine and dried with Na_2SO_4. After being purified by column chromatography and eluting with dichloromethane: methanol = 10: 1. The concentrated product was added to a saturated aqueous solution of ammonium hexafluorophosphate (NH_4PF_6), the suspension was stirred for 1 h, filtered, washed with water and dried. $Ir(ppy)_2(phen)^+$ (**1**) was collected as a yellow-orange solid (124.6 mg, 71.6%). ^{1}H NMR (400 MHz, Acetonitrile-d_3) δ 8.71 (dd, *J* = 8.3, 1.5 Hz, 2H), 8.33 (d, *J* = 3.6 Hz, 2H), 8.26 (s, 2H), 8.08 (d, *J* = 8.2 Hz, 2H), 7.93–7.76 (m, 6H), 7.45 (d, *J* = 4.6 Hz, 2H), 7.11 (t, *J* = 7.5 Hz, 2H), 6.99 (t, *J* = 7.4 Hz, 2H), 6.88 (t, *J* = 6.0 Hz, 2H), 6.42 (d, *J* = 7.7 Hz, 2H).

$Ir(ppy)_2(napphen)^+$ (4). $Ir(ppy)_2(napphen)^+$ (**4**) was obtained as a yellow-orange solid (137.7 mg, 69.1%) according to the same methods as those of **1**, except that 1,10-phenanthrolin was replaced by 4-(2-naphthalenyl)-1,10-phenanthroline. ^{1}H NMR (400 MHz, Chloroform-*d*) δ 8.59 (d, *J* = 8.4 Hz, 2H), 8.31 (d, *J* = 3.7 Hz, 1H), 8.26 (d, *J* = 4.4 Hz, 1H), 8.19 (s, 1H), 8.14 (s, 1H), 7.93 (dd, *J* = 14.6, 7.9 Hz, 5H), 7.79–

7.68 (m, 7H), 7.61–7.54 (m, 3H), 7.41 (d, J = 5.8 Hz, 1H), 7.15–7.03 (m, 3H), 7.00 (t, J = 7.5 Hz, 3H), 6.44 (t, J = 7.4 Hz, 2H). ^{13}C NMR (101 MHz, CD3CN) δ 168.44, 152.08, 152.06, 151.07, 150.77, 150.43, 150.35, 148.28, 147.27, 145.26, 141.75, 139.43, 139.32, 138.17, 135.42, 134.28, 134.09, 132.68, 132.66, 131.92, 131.31, 131.29, 130.27, 129.56, 129.20, 129.16, 128.77, 128.46, 128.06, 127.99, 127.60, 125.82, 124.35, 124.32, 123.57, 120.76. High resolution mass spectrum (HR-MS) for $Ir(ppy)_2(napphen)^{2+}$: calculated m/z 807.2094, observed m/z 807.2050.

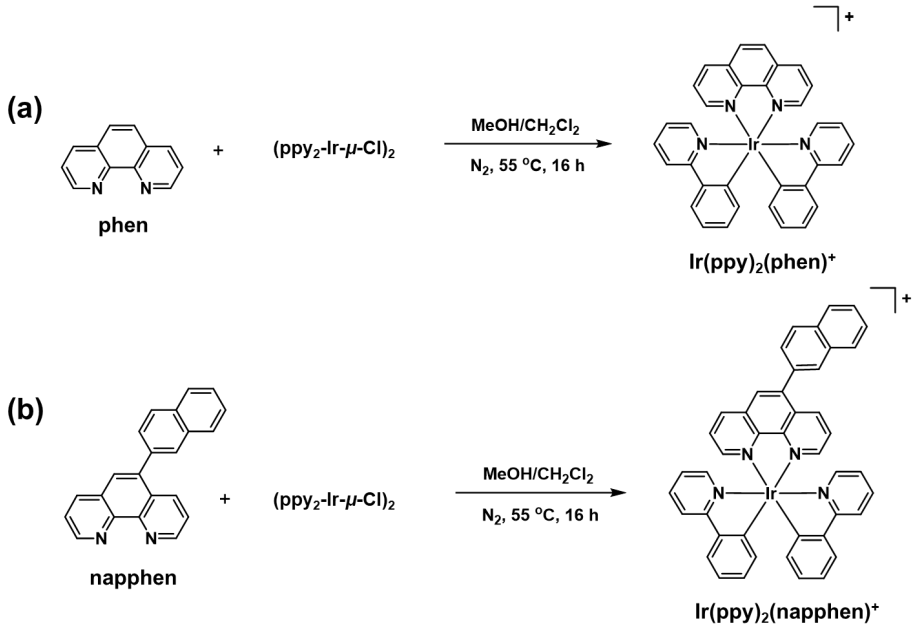

Fig. S3 Illustration of synthesis of Ir(III) complexes (a) $Ir(ppy)_2(phen)^+$ (**1**) and (b) $Ir(ppy)_2(napphen)^+$ (**4**).

S1.4. Synthesis of Ru(II) complexes

$Ru(bpy)_2(phen)^{2+}$ (2). *cis*-$Ru(bpy)_2Cl_2 \cdot 2H_2O$ (0.2 mmol, 104 mg) and 1,10-phenanthroline (0.2 mmol, 36 mg) were added to a mixture of 30 mL of ethanol. The mixture was refluxed at 80℃ for 16 h under the N_2 atmosphere. After being purified by column chromatography and eluting with potassium nitrate: water: acetonitrile = 1: 10: 100. The concentrated product was added to a saturated aqueous solution of ammonium hexafluorophosphate (NH_4PF_6), the suspended was stirred for 1 h, filtered, washed with water and dried. $Ru(bpy)_2(phen)^{2+}$ (**2**) was collected as a red solid (130.8 mg, 74.0%). ^{1}H NMR (400 MHz, Acetonitrile-d_3) δ 8.63 (d, J = 8.3 Hz, 2H), 8.54 (dd, J = 17.3, 8.2 Hz, 4H), 8.26 (s, 2H), 8.14 – 8.08 (m, 4H), 8.00 (t, J = 7.9 Hz, 2H), 7.86 (d, J = 5.4 Hz, 2H), 7.75 (dd, J = 8.3, 5.2 Hz, 2H), 7.54 (d, J = 5.4 Hz, 2H), 7.46 (t, J = 6.6 Hz, 2H), 7.23 (t, J = 6.3 Hz, 2H).

$Ru(bpy)_3^{2+}$ (3). $Ru(bpy)_3^{2+}$ was collected as a red solid (132.4 mg, 73.2%) by the similar synthesis steps of **2**, expect that 1,10-phenanthroline was replaced by 2,2′-bipyridine. ^{1}H NMR (400 MHz, Acetonitrile-d_3) δ 8.56 (d, J = 8.1 Hz, 6H), 8.08 (td, J = 7.9, 1.5 Hz, 6H), 7.74 (d, J = 5.6 Hz, 6H), 7.41 (ddd, J = 7.4, 5.6, 1.3 Hz, 6H).

Ru(bpy)$_2$(napphen)$^{2+}$ (5). Ru(bpy)$_2$(napphen)$^{2+}$ (**5**) was collected as a red solid (146.5 mg, 69.5%) by the similar synthesis steps of **2**, expect that 1,10-phenanthroline was replaced by 4-(2-naphthalenyl)-1,10-phenanthroline. ^{1}H NMR (400 MHz, Acetonitrile-d_3) δ 8.66 (d, J = 8.2 Hz, 1H), 8.63–8.52 (m, 5H), 8.34 (s, 1H), 8.20–8.11 (m, 6H), 8.11–8.02 (m, 4H), 7.90 (d, J = 5.6 Hz, 2H), 7.83–7.76 (m, 2H), 7.67 (ddt, J = 15.9, 10.2, 4.5 Hz, 5H), 7.49 (t, J = 5.7 Hz, 2H), 7.30 (dt, J = 6.4, 4.6 Hz, 2H). ^{13}C NMR (101 MHz, CD3CN) δ 158.22, 158.18, 157.98, 153.27, 152.92, 152.84, 149.01, 148.04, 141.68, 138.79, 138.77, 138.69, 138.67, 137.61, 136.56, 135.43, 134.26, 134.08, 131.42, 131.39, 130.25, 129.55, 129.18, 129.00, 128.75, 128.48, 128.44, 128.39, 128.35, 128.05, 127.99, 127.32, 126.82, 125.21, 125.19, 125.13. HR-MS for Ru(bpy)$_2$(napphen)$^{2+}$: calculated m/z 360.0782, observed m/z 360.0773.

Ru(bpy)$_2$(napbpy)$^{2+}$ (6). Ru(bpy)$_2$(napbpy)$^{2+}$ (**6**) was prepared as a red solid (134.3 mg, 65.2%) by the similar synthesis steps of **2**, except that 1,10-phenanthroline was replaced by 4-(2-naphthalenyl)-2,2′-bipyridine. ^{1}H NMR (400 MHz, Acetonitrile-d_3) δ 8.91 (s, 1H), 8.76 (d, J = 8.1 Hz, 1H), 8.55 (dd, J = 8.2, 5.3 Hz, 4H), 8.48 (d, J = 1.9 Hz, 1H), 8.14–8.05 (m, 7H), 8.02–7.96 (m, 2H), 7.86 (d, J = 4.9 Hz, 1H), 7.82–7.76 (m, 6H), 7.66–7.61 (m, 2H), 7.47–7.40 (m, 5H). ^{13}C NMR (101 MHz, CD3CN) δ 158.36, 158.08, 157.96, 157.92, 152.66, 152.62, 152.60, 150.31, 138.76, 138.70, 134.92, 134.29, 133.87, 130.20, 129.64, 128.71, 128.68, 128.60, 128.55, 128.52, 128.43, 128.13, 125.88, 125.40, 125.22, 125.12, 122.97. HR-MS for Ru(bpy)$_2$(napbpy)$^{2+}$: calculated m/z 348.0782, observed m/z 348.0777.

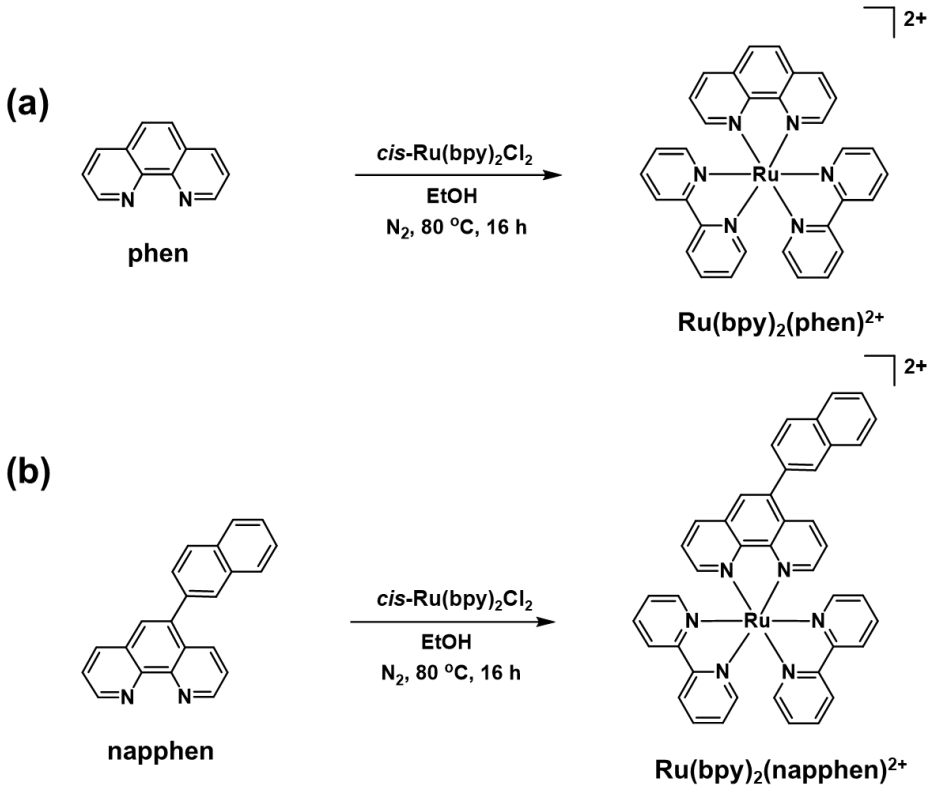

Fig. S4 Illustration of synthesis of Ru(II) complexes (a) Ru(bpy)$_2$(phen)$^{2+}$ (**2**) and (b) Ru(bpy)$_2$(napphen)$^{2+}$ (**5**).

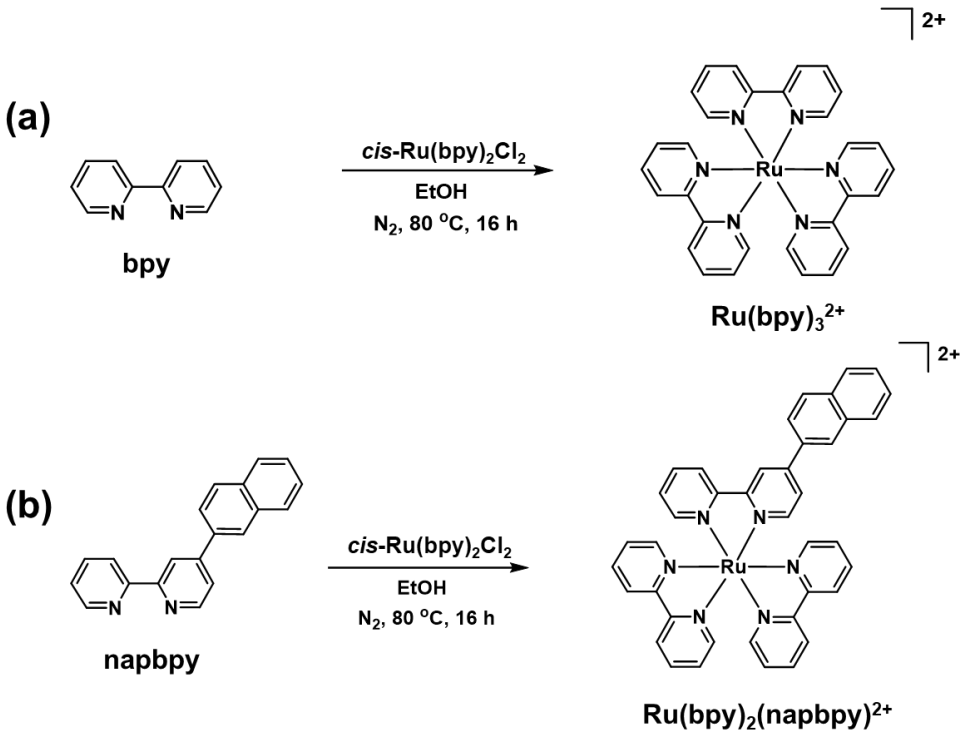

Fig. S5 Illustration of synthesis of Ru(II) complexes (a) $Ru(bpy)_3^{2+}$ (**3**) and (b) $Ru(bpy)_2(napbpy)^{2+}$ (**6**).

S2. ^{1}H NMR Characterization of 1-6

^{1}H NMR characterization of the synthesized compounds was carried out on a 400 MHz spectrometer (Bruker, Germany) and presented in **Fig. S6**.

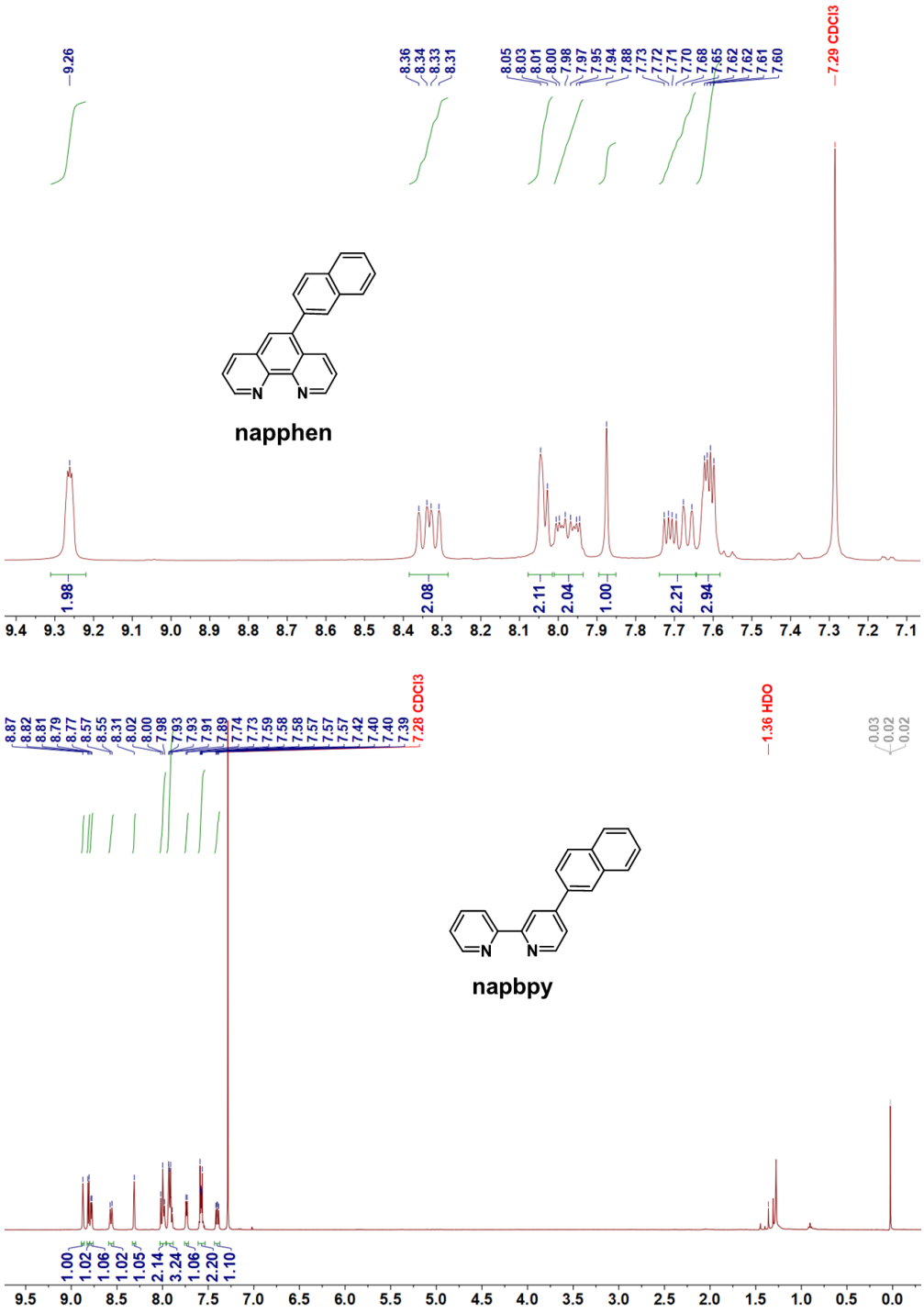

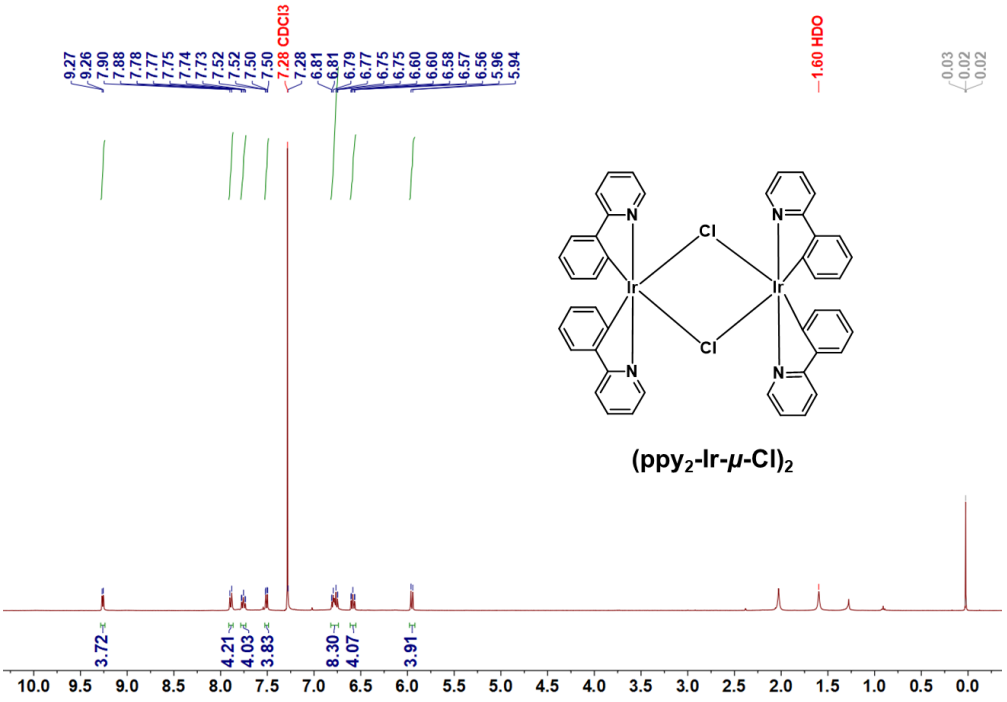

$(ppy_2\text{-}Ir\text{-}\mu\text{-}Cl)_2$

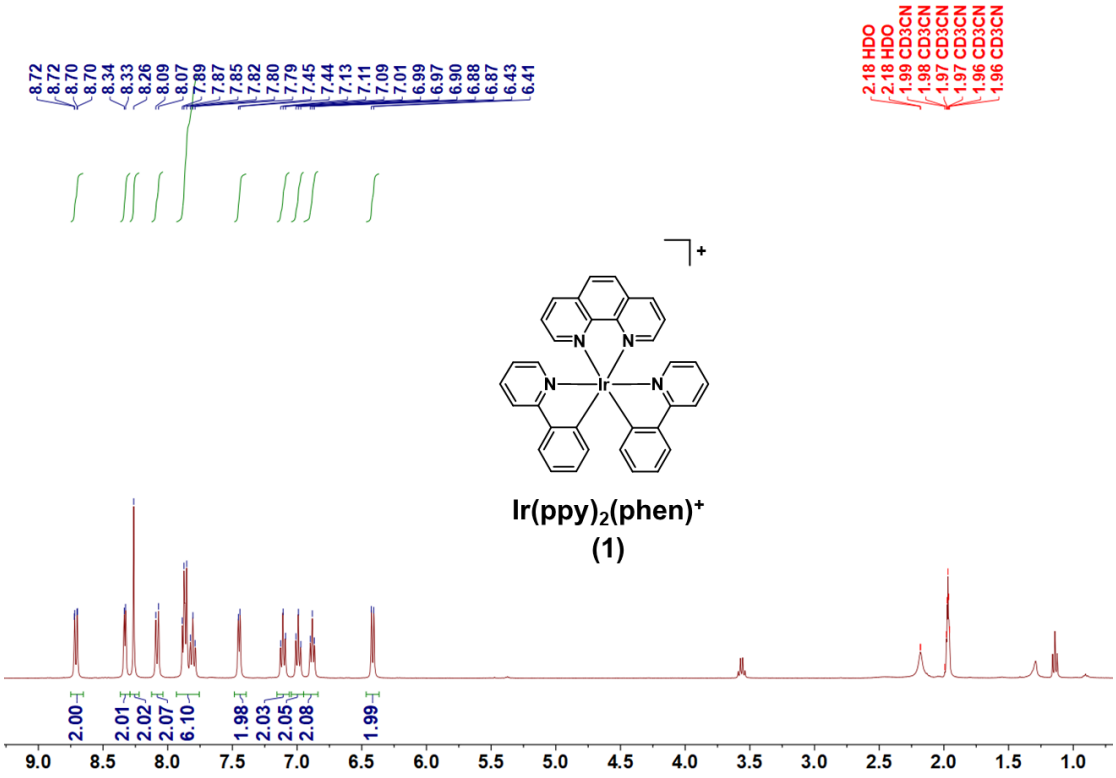

$Ir(ppy)_2(phen)^+$
(1)

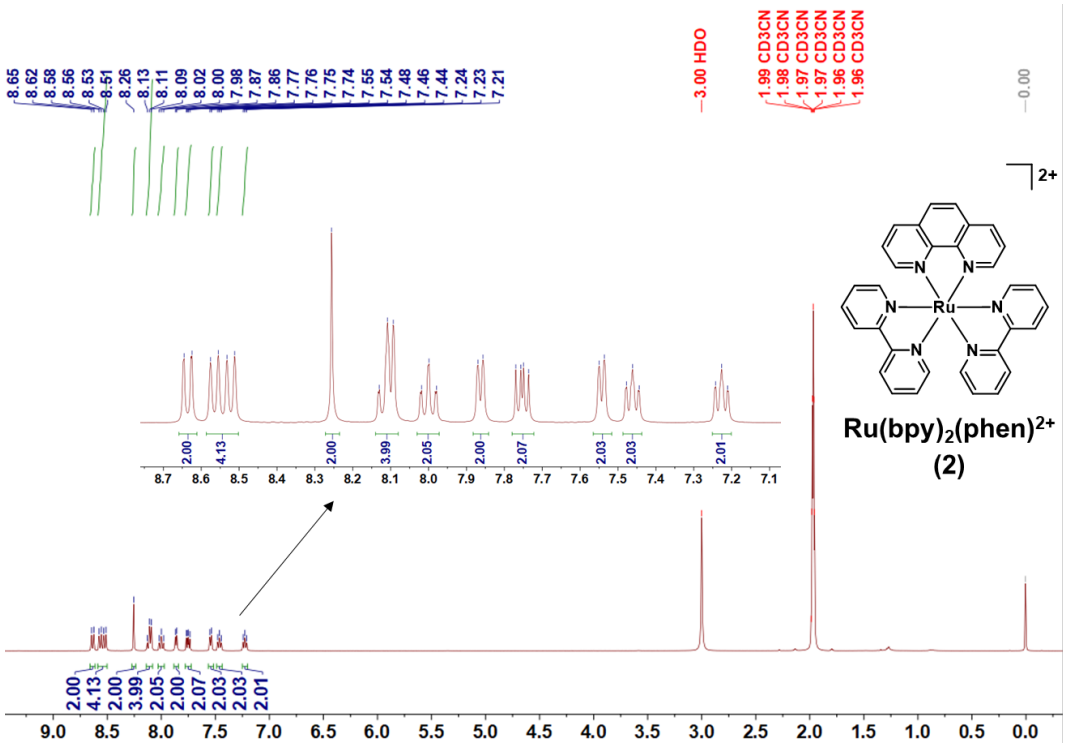
8.65
8.62
8.58
8.56
8.53
8.51
8.26
8.13
8.11
8.09
8.02
8.00
7.98
7.87
7.86
7.77
7.76
7.75
7.74
7.55
7.54
7.48
7.46
7.44
7.24
7.23
7.21
3.00 HDO
1.99 CD3CN
1.98 CD3CN
1.97 CD3CN
1.97 CD3CN
1.96 CD3CN
1.96 CD3CN
0.00
2+
Ru(bpy)2(phen)2+
(2)
2.00
4.13
2.00
3.99
2.05
2.00
2.07
2.03
2.03
2.01

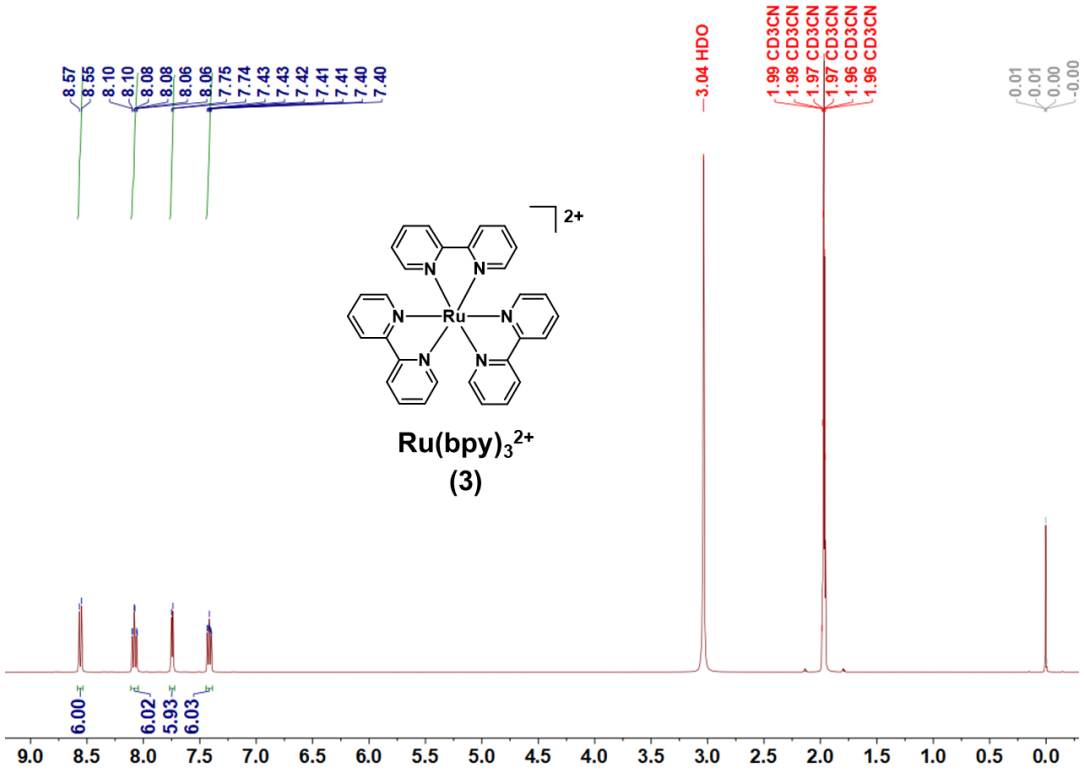
8.57
8.55
8.10
8.10
8.08
8.08
8.06
8.06
7.75
7.74
7.43
7.42
7.41
7.41
7.40
7.40
3.04 HDO
1.99 CD3CN
1.98 CD3CN
1.97 CD3CN
1.97 CD3CN
1.96 CD3CN
1.96 CD3CN
0.01
0.01
0.00
-0.00
2+
Ru(bpy)3 2+
(3)
6.00
6.02
5.93
6.03

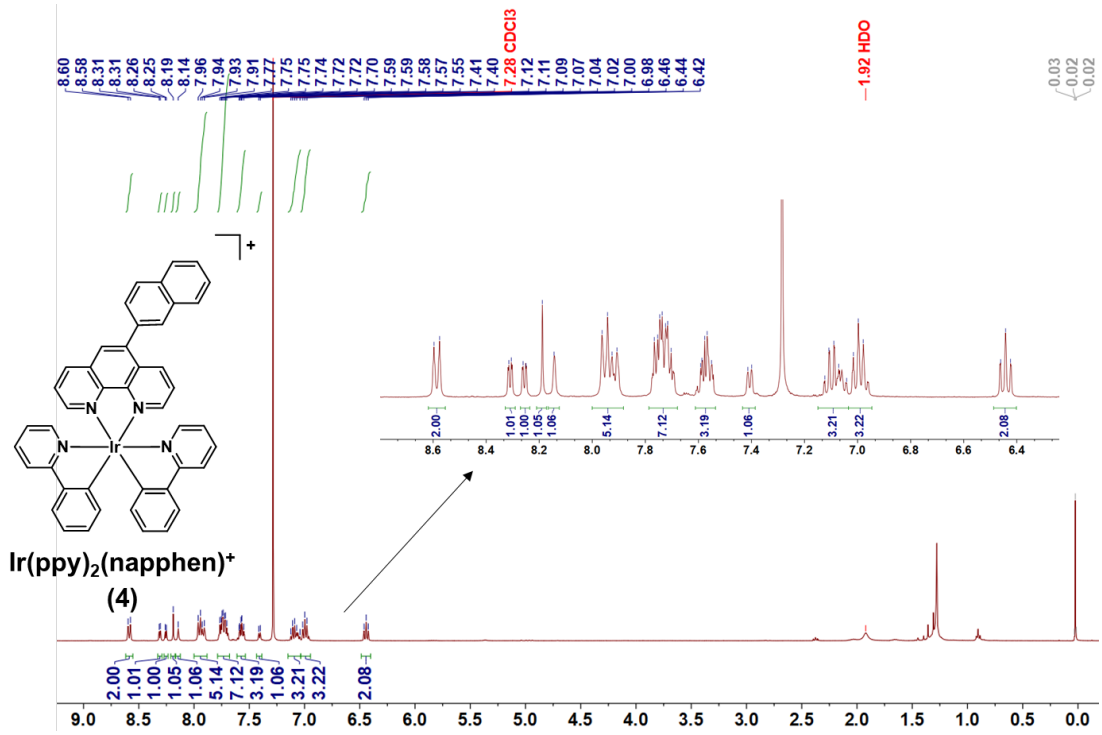
8.60 8.58 8.31 8.31 8.26 8.25 8.19 8.14 7.96 7.94 7.93 7.91 7.77 7.75 7.74 7.72 7.72 7.70 7.59 7.59 7.58 7.57 7.55 7.41 7.40 7.28 CDCl3 7.12 7.11 7.09 7.07 7.04 7.02 7.00 6.98 6.46 6.44 6.42
1.92 HDO
0.03 0.02 0.02
+
N N N Ir N N
Ir(ppy)2(napphen)+
(4)
2.00 1.01 1.00 1.05 1.06 5.14 7.12 3.19 1.06 3.21 3.22 2.08
9.0 8.5 8.0 7.5 7.0 6.5 6.0 5.5 5.0 4.5 4.0 3.5 3.0 2.5 2.0 1.5 1.0 0.5 0.0

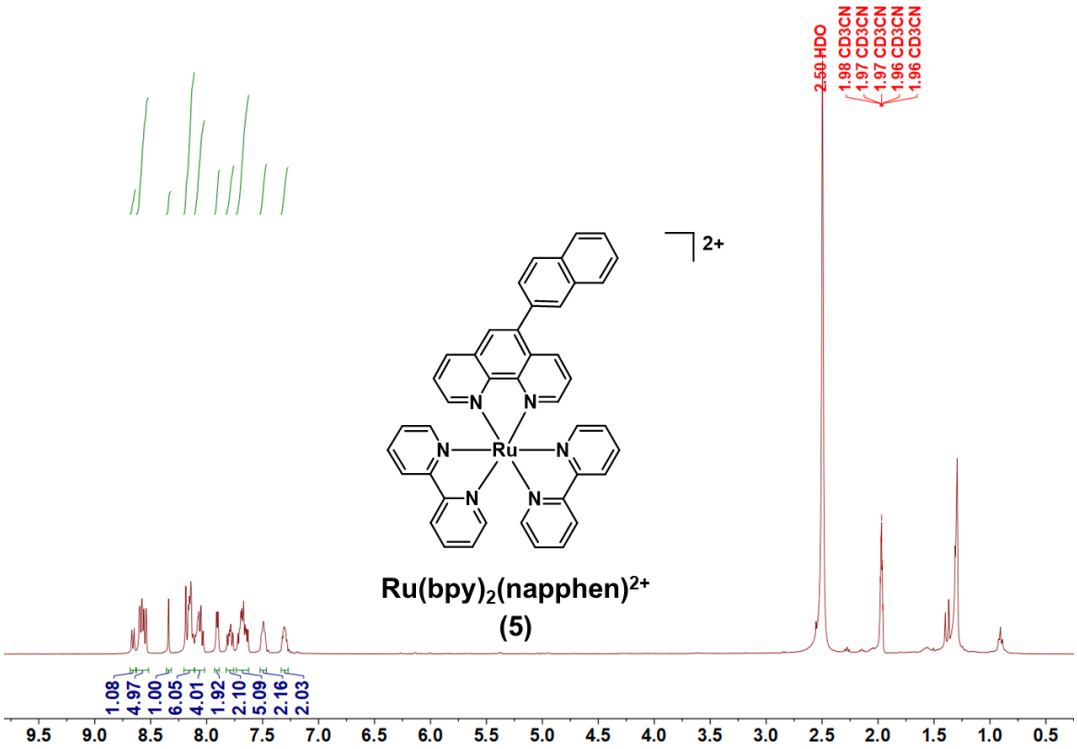
2.50 HDO
1.98 CD3CN 1.97 CD3CN 1.97 CD3CN 1.96 CD3CN 1.96 CD3CN
2+
N N N Ru N N N N
Ru(bpy)2(napphen)2+
(5)
1.08 4.97 1.00 6.05 4.01 1.92 2.10 5.09 2.16 2.03
9.5 9.0 8.5 8.0 7.5 7.0 6.5 6.0 5.5 5.0 4.5 4.0 3.5 3.0 2.5 2.0 1.5 1.0 0.5

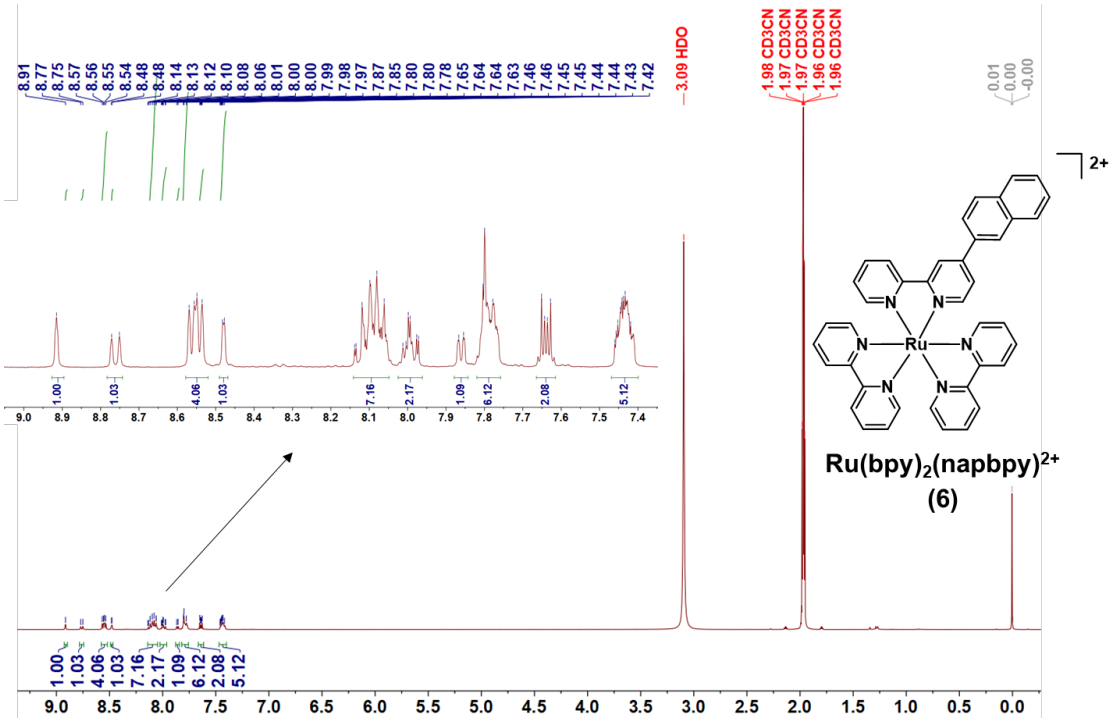

Fig. S6 ^{1}H NMR spectra of two types of ancillary ligands (N^N) napphen and napbpy, bis *m*-chloro dinuclear Ir(III) complex (ppy_2-Ir-*m*-Cl_2, Ir(III)/Ru(II) complexes $Ir(ppy)_2(phen)^+$ (**1**), $Ru(bpy)_2(phen)^{2+}$ (**2**), $Ru(bpy)_3^{2+}$ (**3**), $Ir(ppy)_2(napphen)^+$ (**4**), $Ru(bpy)_2(napphen)^{2+}$ (**5**), and $Ru(bpy)_2(napbpy)^{2+}$ (**6**). Insets show the molecular structures.

S3. ^{13}C NMR Characterization of 4/5/6

^{13}C NMR characterization of the synthesized compounds were carried out on a 400 MHz spectrometer (Bruker, Germany) and presented in **Fig. S7**.

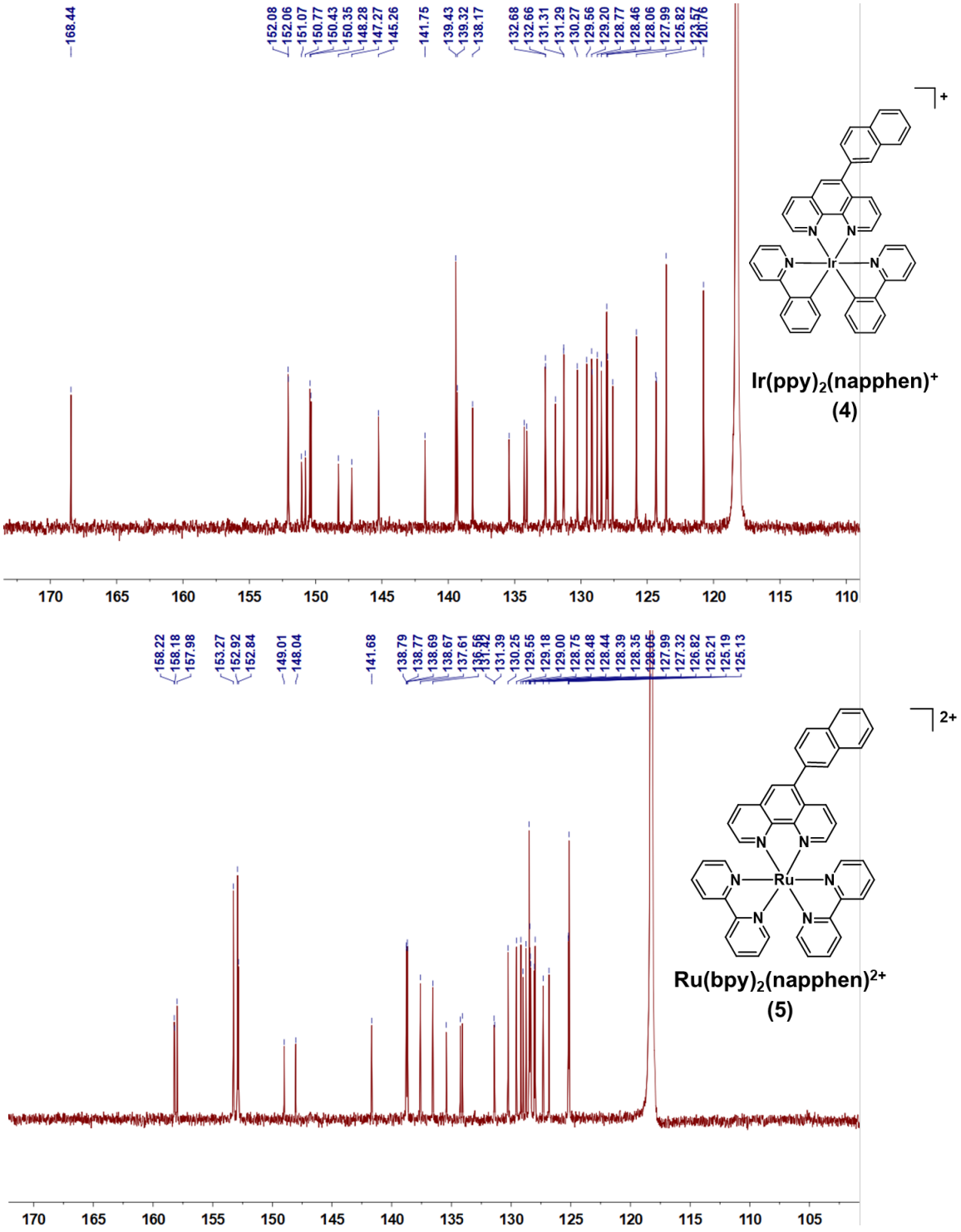

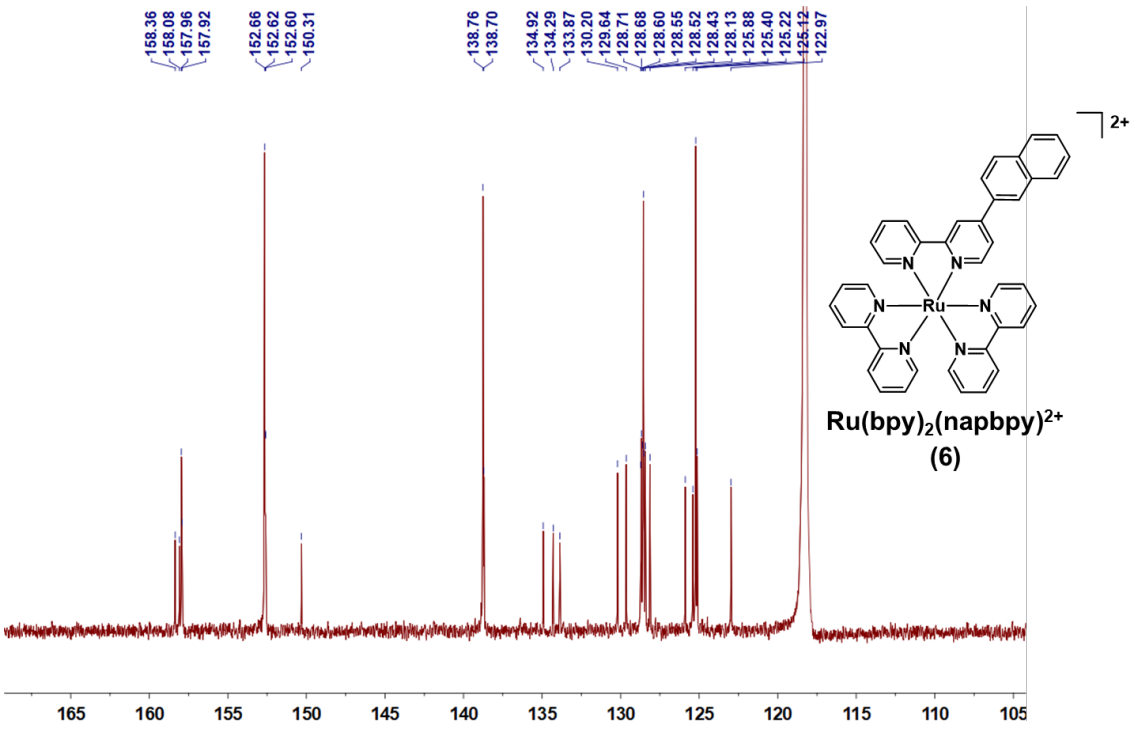

Fig. S7 ^{13}C NMR spectra of Ir(ppy)$_2$(napphen)$^+$ (**4**), Ru(bpy)$_2$(napphen)$^{2+}$ (**5**), and Ru(bpy)$_2$(napbpy)$^{2+}$ (**6**). Insets show the molecular structures.

S4. High Resolution Mass Spectra of 4/5/6

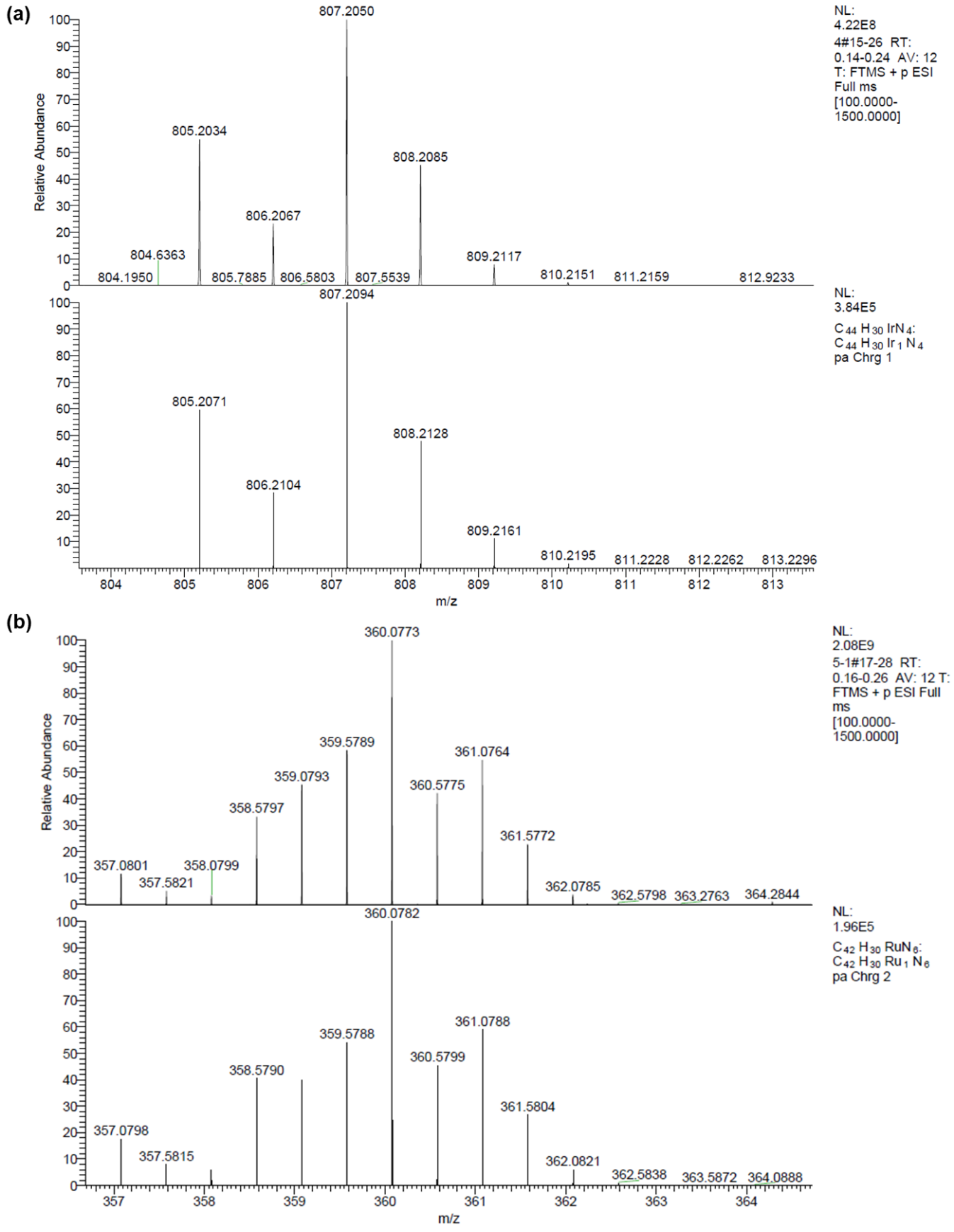

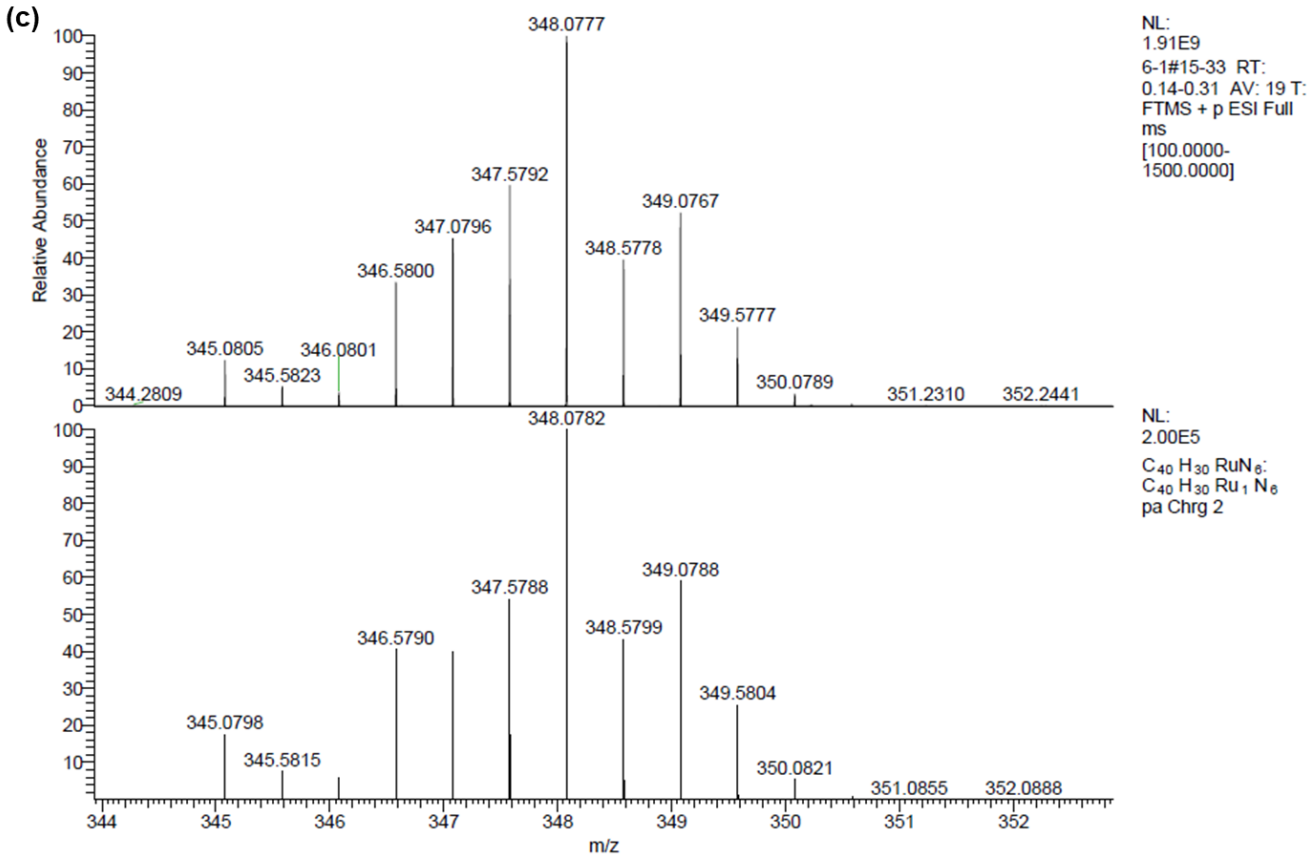

Fig. S8 High resolution mass spectra of metal complexes, **4** (a), **5** (b), and **6** (c). The measurement (top) and calculation (bottom) data were obtained with a Q Exactive Orbitrap Mass Spectrometer (ThermoFisher).

S5. ECL Performance of 1/2/3/4/6

Fig. S9 indicates the ECL intensity-potential curves overlaid with CVs of **1**/**2**/**3**/**4**/**6** obtained in acetonitrile containing 0.1 M $TBAPF_6$ and 50 mM TPrA. The concentrations of these complexes were 10 mM. The ECL intensity of these complexes increased as the oxidation potential was increased. Moreover, the intensity follows the order of **5** > **1** > **6** > **3** > **4** > **2**. That is, **5** is the most efficient ECL luminophore among these six complexes. This result can be further confirmed by spooling ECL spectra (**Fig. S10**).

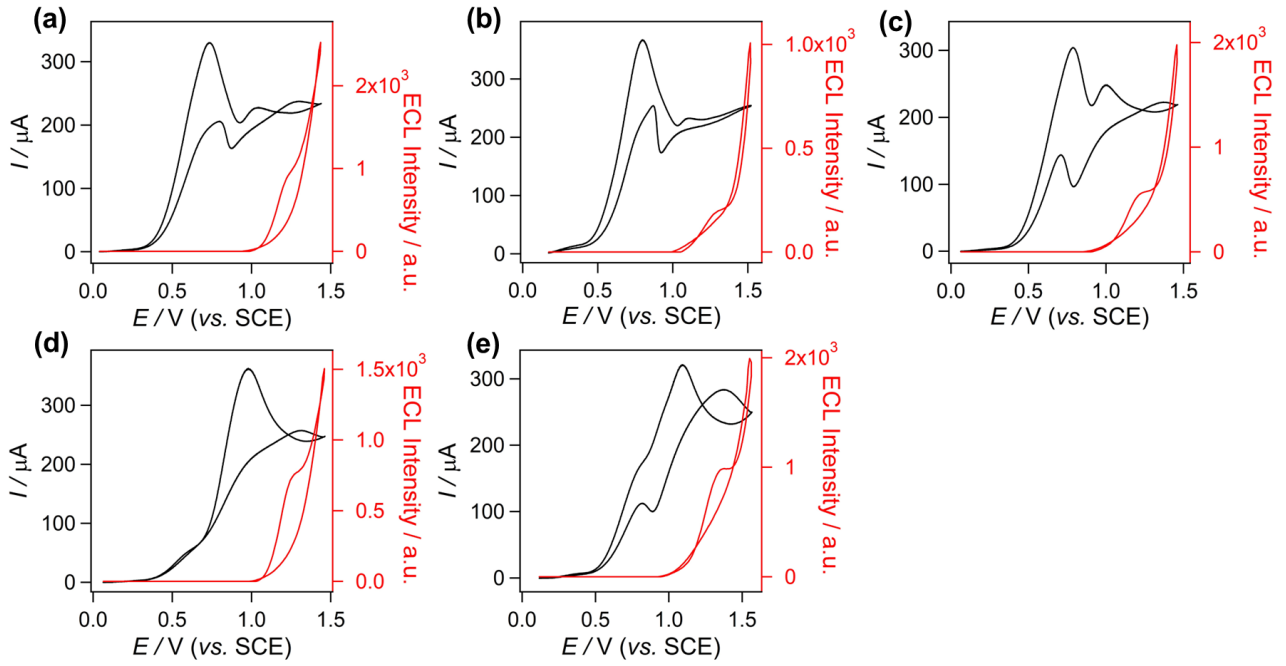

Fig. S9 (a-e) ECL intensity-potential curves overlaid with CVs of **1**/**2**/**3**/**4**/**6** (10 mM) dissolved in acetonitrile containing 50 mM TPrA and 0.1 M $TBAPF_6$. The photomultiplier tube (PMT) was biased at 400 V. The scan rate was 0.1 V s^{-1}.

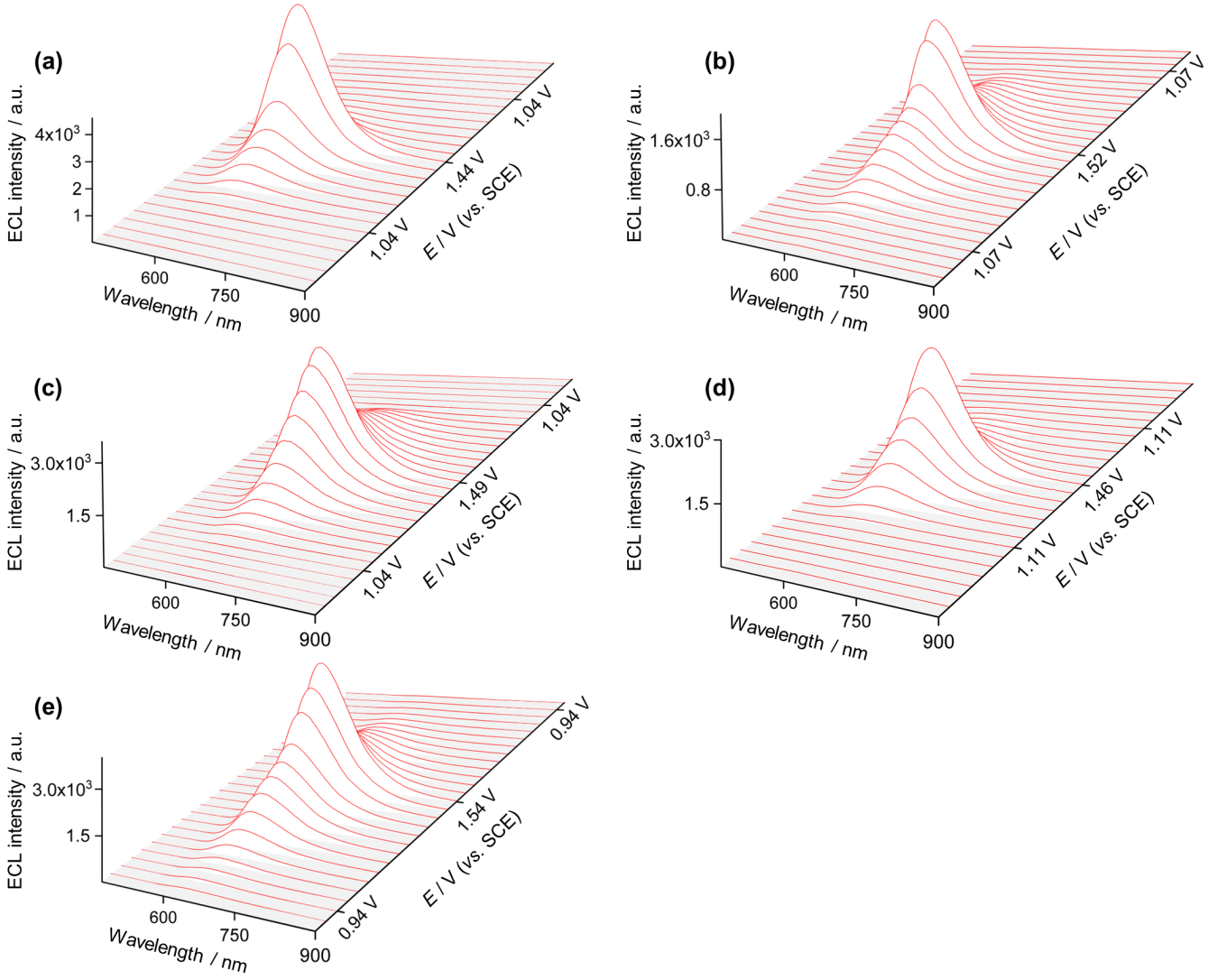

Fig. S10 (a-e) Spooling ECL spectra of **1/2/3/4/6** (500 mM) dissolved in acetonitrile containing 50 mM TPrA and 0.1 M $TBAPF_6$. The scan rate was 0.1 V s^{-1}. The spectral integration time was 0.5 s, and two adjacent spectra were obtained at potential intervals of 50 mV. **1/2/3/4/6** presents the ECL spectrum at formal oxidation voltage of +1.44 V, +1.52 V, +1.49 V, +1.46 V, and +1.54 V, respectively.

S6. ECL Efficiencies (Φ_{ECL})

The Φ_{ECL} of **1-6** was measured as photons emitted per oxidation event,[S5] which were calculated by comparing both the integrated ECL intensities (equivalent to the number of photons) and the current values (same as charges) vs time with that of the reference $Ru(bpy)_3^{2+}$/TPrA, using the equation as follows:[S1, S6]

$$\Phi_{ECL} = \left(\frac{\int_0^t ECL\,\mathrm{d}t}{\int_0^t Current\,\mathrm{d}t}\right)_x \Big/ \left(\frac{\int_0^t ECL\,\mathrm{d}t}{\int_0^t Current\,\mathrm{d}t}\right)_{st} \quad \text{(S1)}$$

where Φ is the ECL efficiency relative to $Ru(bpy)_3(PF_6)_2$, whose ECL efficiency is taken as 1, *x* represents complex **1-6**, *ECL* represents the ECL intensity, *current* is the electrochemical current value, and st means the standard.

The current-time and ECL intensity-time curves of **1-6** were obtained by MPI-A capillary electrophoresis-electrochemiluminescence analyzer. The potential window was set from 0 V to about 100 mV higher than the oxidation peak potential for each complex, which was ca. +1.44 V, +1.52 V, +1.49 V, +1.46 V, +1.52 V, and +1.54 V (vs SCE), respectively. The PMT was biased at 400 V and the scan rate was 0.1 V s^{-1}. By the equation of $Q = \int_0^t Current\,\mathrm{d}t$ and $ECL = \int_0^t ECL\,\mathrm{d}t$, electric charges (Q) and ECL intensities (ECL) were obtained. As illustrated in **Fig. S11**, the area of shaded parts represents the integral of Q, which was calculated as 2258.9, 2473.6, 2046.7, 2078.1, 1693.4, and 2177.7 μC for **1-6**, respectively. While the area that stands for the integral of ECL in **Fig. S13** was calculated to be 3797.0, 1013.8, 2901.8, 2625.5, 4271.0, and 3765.0, respectively (see **Table S1**). After dividing ECL by Q, the Φ_{ECL} was determined with that of $Ru(bpy)_3^{2+}$/TPrA and summarized in **Table 1**. Taking both electrochemical reactions and emission processes, **5** ultimately gives efficient emission with the highest value of Φ_{ECL} that obtained as 1.78. After removing O_2, the area of shaded parts represents the integral of Q, which was calculated as 2258.9, 2473.6, 2046.7, 2078.1, 1693.4, and 2177.7 μC for **1-6**, respectively (see **Fig. S12)**. While the area that stands for the integral of ECL in **Fig. S14** was calculated to be 38870.5, 5758.6, 5202.4, 8157.6, 16400.8 and 16646.1, respectively (see **Table S1**). After dividing ECL by Q, the Φ_{ECL} was determined with that of $Ru(bpy)_3^{2+}$/TPrA.

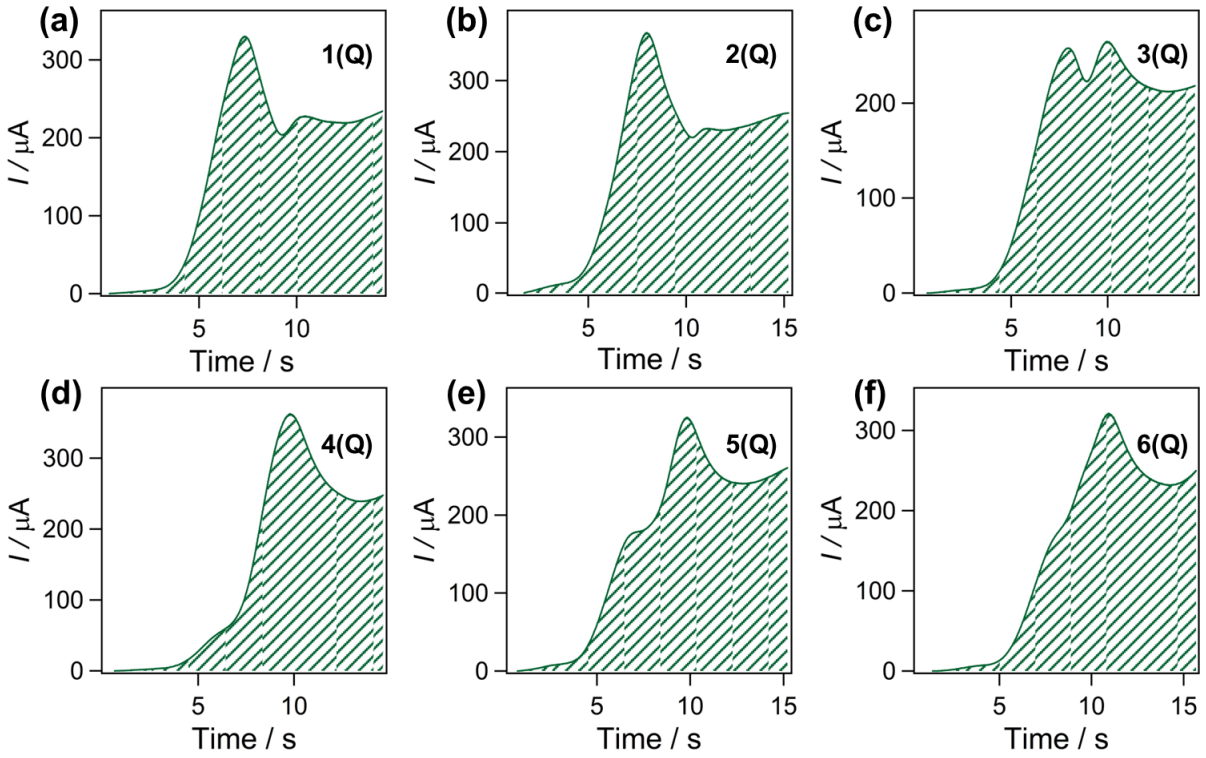

Fig. S11 Current-time curves of **1-6**. The experiment was conducted in acetonitrile containing 10 mM of **1-6**, 50 mM of TPrA and 0.1 M $TBAPF_6$.

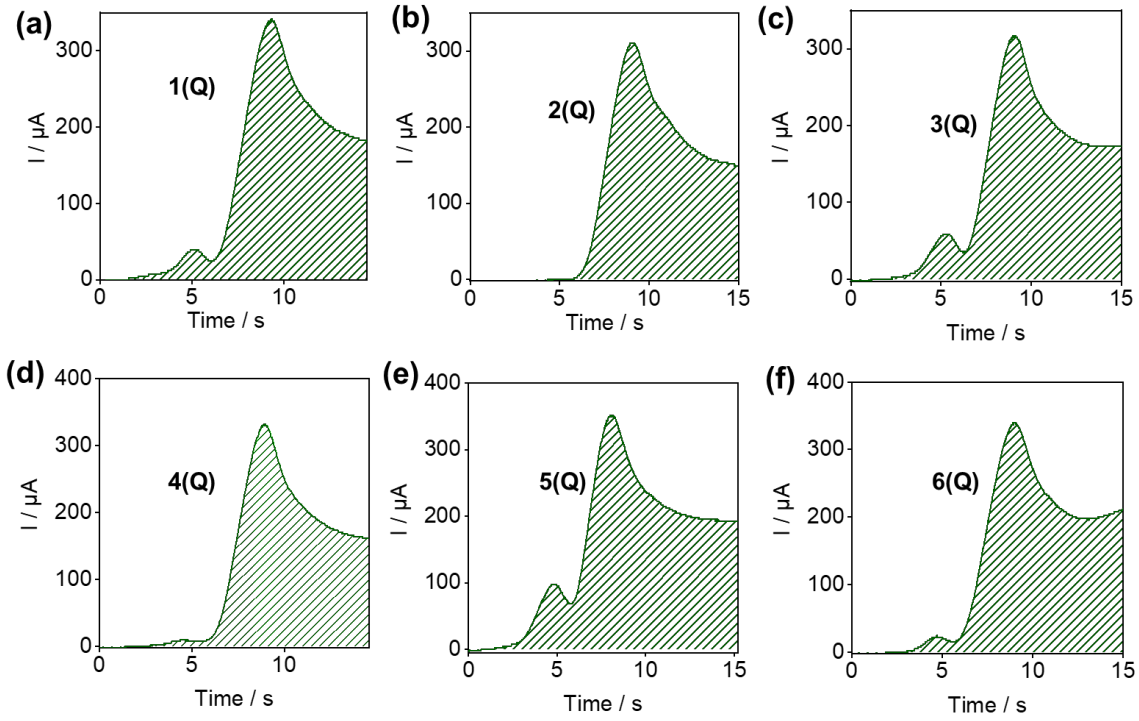

Fig. S12 Current-time curves of **1-6**. The experiment was conducted in acetonitrile containing 10 mM of **1-6**, 50 mM of TPrA and 0.1 M $TBAPF_6$ without O_2.

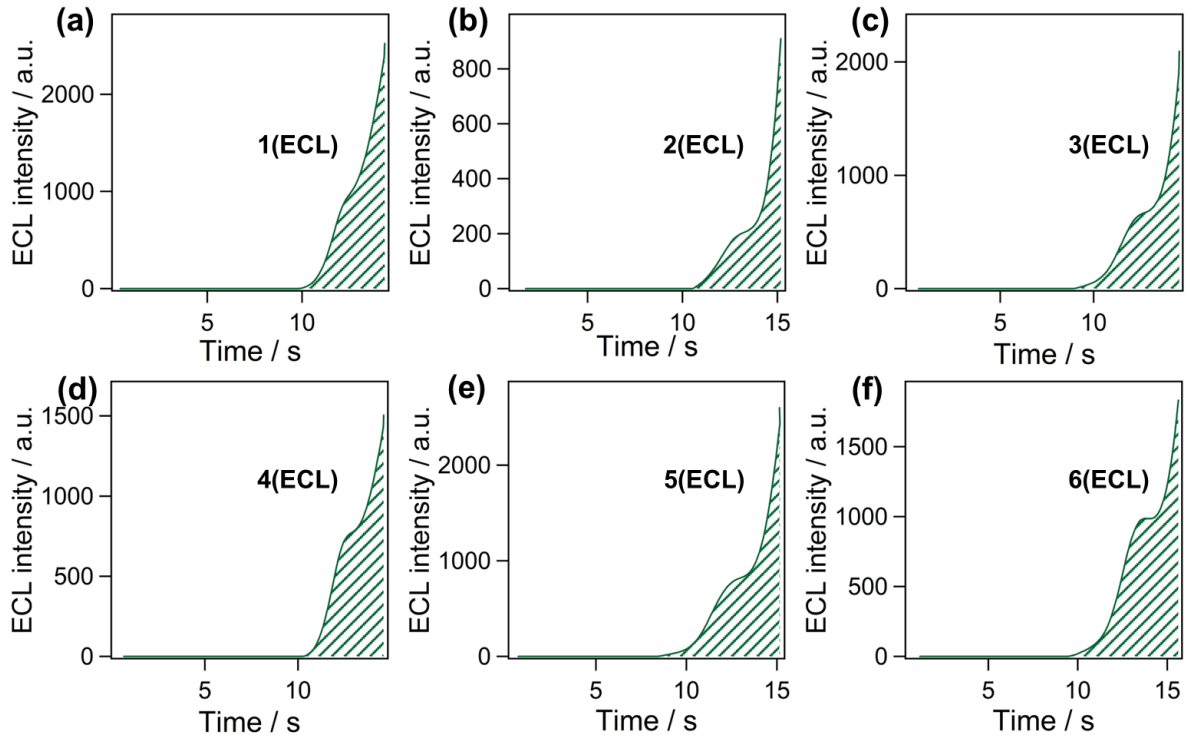

Fig. S13 ECL intensity-time curves of **1-6**. The experiment was conducted in acetonitrile containing 10 mM of **1-6**, 50 mM of TPrA and 0.1 M $TBAPF_6$ in nitrogen-saturated acetonitrile solution.

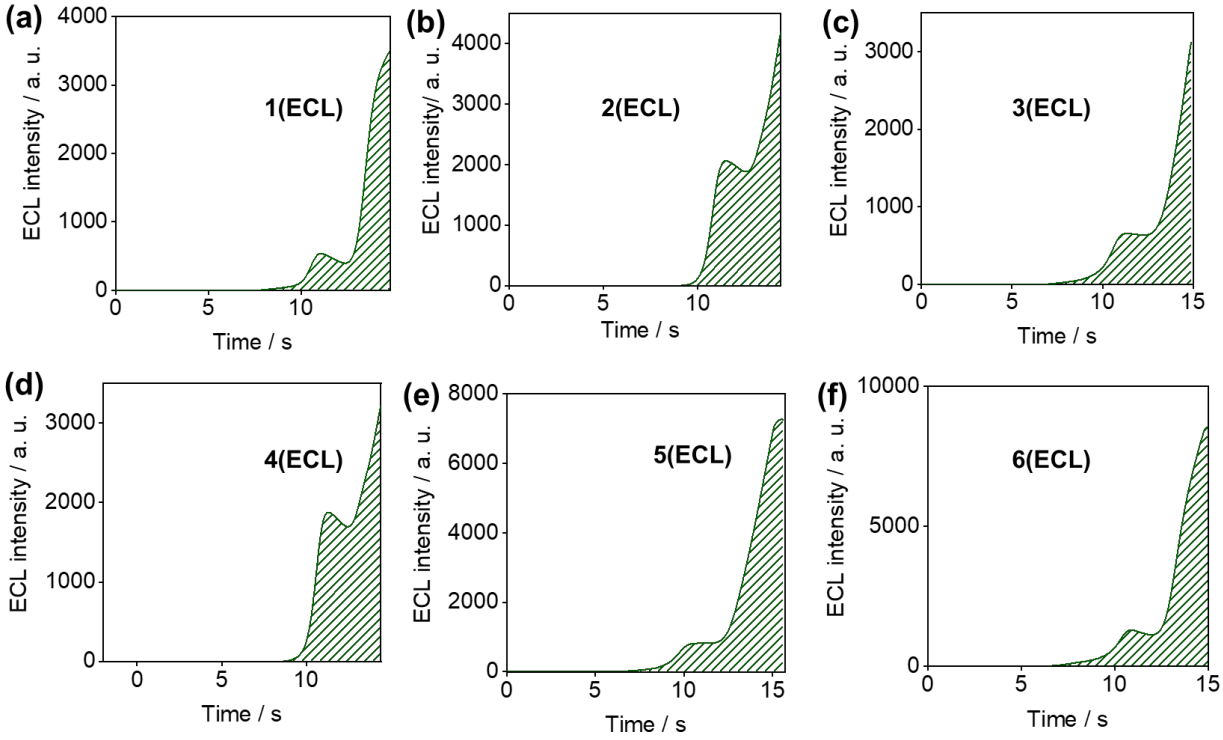

Fig. S14 ECL intensity-time curves of **1-6**. The experiment was conducted in acetonitrile containing 10 mM of **1-6**, 50 mM of TPrA and 0.1 M $TBAPF_6$ in nitrogen-saturated acetonitrile solution.

Table S1. Calculation of ECL QE by integrating both ECL intensities and the current values vs time

Probe	$\int_0^t ECL\ \mathrm{d}t$	$\int_0^t Current\ \mathrm{d}t\ (m\mathrm{C})$
1	3797.0[b]/8870.5[c]	2258.9[d]/1847.2[e]
2	1013.8/5758.6	2473.6/1624.4
3	2901.8/5202.4	2046.7/1824.8
4	2625.5/8157.6	2078.1/1689.9
5	4271.0/16400.8	1693.4/2302.3
6[a]	3765.0/16646.1	2177.7/1968.1

[a]The Φ_{ECL} of $Ru(bpy)_3^{2+}$/TPrA was set to 1.00 as a standard. [b, c]Integration of ECL intensities obtained in aerated and nitrogen-saturated acetonitrile solution, respectively. [d, e]Integration of the electrochemical current obtained in aerated and nitrogen-saturated acetonitrile solution, respectively.

S7. Fluorescence Titration Experiment

Fluorescence titrations were performed to confirm the formation of a host-guest complex (HGC) between 6-deoxy-6-thiol-*β*-cyclodextrin (*β*-CD-SH) and **5**. 10 μM of **5** was dissolved in DMSO/H_2O (v/v: 1/1) solution while nearly saturated *β*-CD-SH (ca. 75.23 mM) in pure DMSO solution was gradually added in microliters. Fluorescence spectra of **5** via different concentrations of *β*-CD-SH were recorded. The data of each fluorescence intensity centred at the maximum wavelength as well as corresponding concentration of *β*-CD-SH were extracted, and a binding constant of HGC was determined by the modified Benesi-Hildebrand equation,[S7]

$$\frac{[G][H]}{F\text{-}F_0} = \left(\frac{1}{K\alpha} + \frac{[H]}{\alpha}\right) \quad \text{(S2)}$$

where [G] and [H] represents the concentration of **5** and *β*-CD-SH, respectively. ($F\text{-}F_0$) is the change value relative to pure **5** (F_0) in fluorescence intensity with the addition of *β*-CD-SH. *α* is the sensitive factor of fluorescence spectrum. K stands for the binding constant of the supramolecular system.

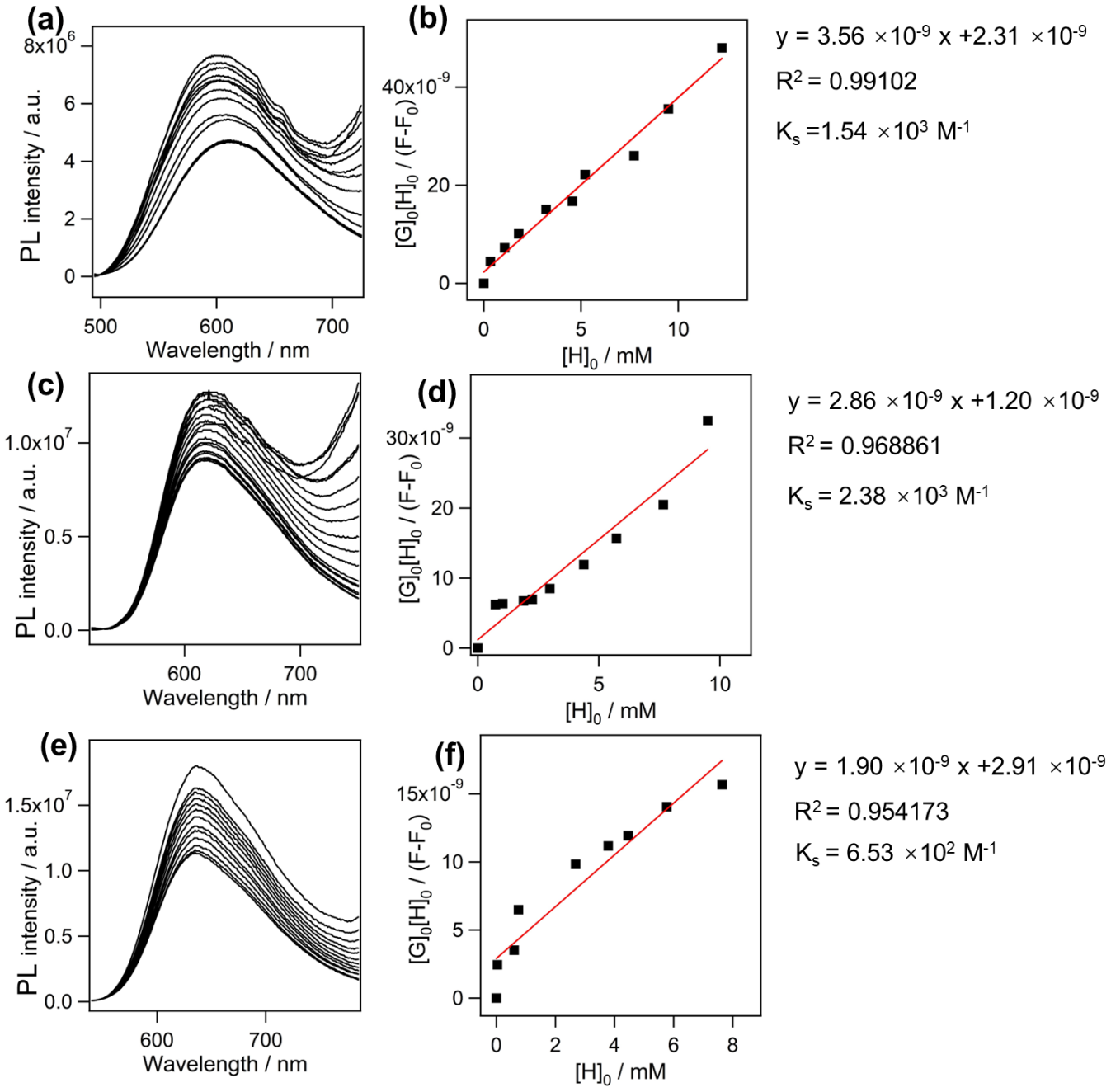

Fig. S15 (a, c, e) PL spectra and (b, d, f) dependence of PL intensity on the host concentrations for **4** (a, b), **5** (c, d) and **6** (e, f) in a DMSO/H_2O (v/v: 1/1) solution, showing an increase in PL intensity with increasing concentrations of β-CD-SH. An excitation wavelength of 450 nm was used. The concentration of **4-6** was 10 μM.

S8. XPS Characterization of Host-Guest Thin Film

A sputter coater (GVC-2000T) was used to deposit gold layer on the substrate with a thickness of ca. 200 nm. A working current of 60 mA and a working time of 20 min were used. The prepared gold membrane electrode was used to fabricate host-guest thin film.

As shown in **Fig. S14**, XPS signals of N and S elements were recorded with the gold thin films. In the XPS spectra, the signals of N1s and S2p can simultaneously be identified for host-guest thin film, while only S2p can be observed for *β*-CD film. While no obvious XPS signal was observed for the bare gold electrode.

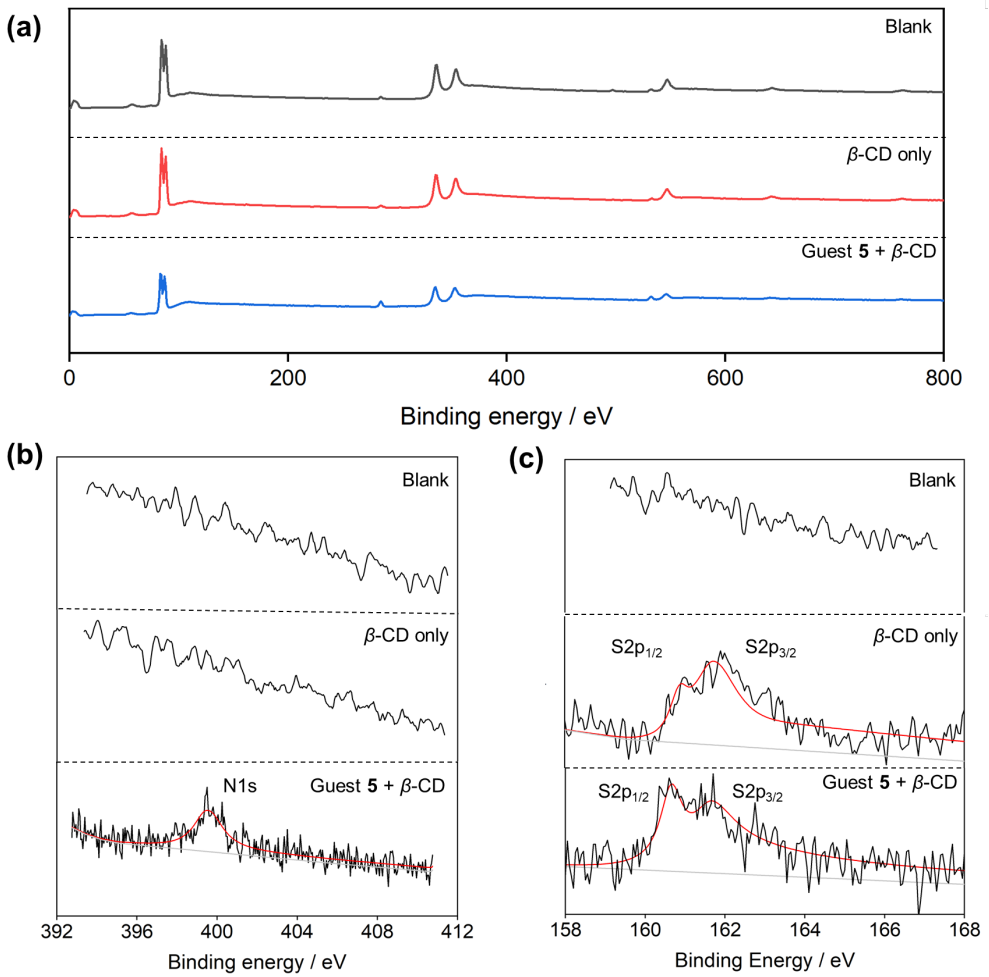

Fig. S16 (a) XPS survey spectra and high-resolution (b) N1s and (c) S2p spectra of the bare gold thin film, *β*-CD modified and host-guest thin film modified gold thin films.

S9. ECL Generation from Host-Guest Thin Films

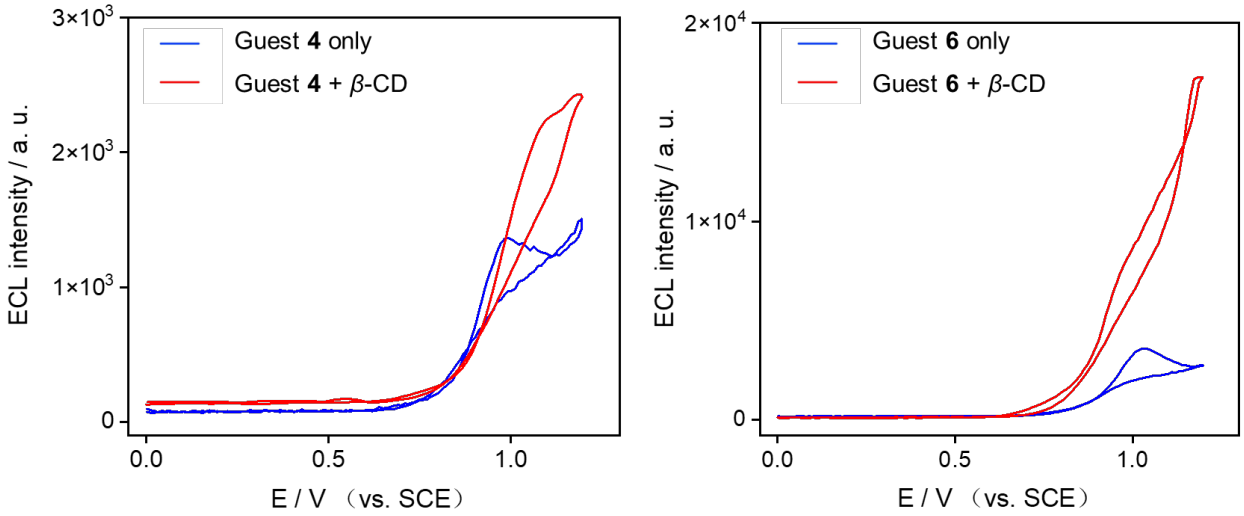

Fig. S17 ECL intensity-potential curves obtained with gold electrode without *β*-CD-SH treatment (blue line), and host-guest thin films modified gold electrode (red line).

References

S1. X. Yang, Y. Xu, X. Huang, J. Hang, W. Guo and Z. Dai, *Anal. Chem.*, 2023, **95**, 4543-4549.

S2. R. Lincoln, L. Kohler, S. Monro, H. Yin, M. Stephenson, R. Zong, A. Chouai, C. Dorsey, R. Hennigar, R. P. Thummel and S. A. McFarland, *J. Am. Chem. Soc.*, 2013, **135**, 17161-17175.

S3. M. Mydlak, C. Bizzarri, D. Hartmann, W. Sarfert, G. Schmid and L. De Cola, *Adv. Funct. Mater.*, 2010, **20**, 1812-1820.

S4. B. Yang, P. Tao, C. Ma, R. Tang, T. Gong, S. Liu and Q. Zhao, *J. Mater. Chem. C*, 2020, **8**, 5449-5455.

S5. W. Guo, H. Ding, C. Gu, Y. Liu, X. Jiang, B. Su and Y. Shao, *J. Am. Chem. Soc.*, 2018, **140**, 15904-15915.

S6. M. Hesari, J. S. Lu, S. Wang and Z. Ding, *Chem. Commun.*, 2015, **51**, 1081-1084.

S7. H. A. Benesi and J. Hildebrand, *J. Am. Chem. Soc.*, 1949, **71**, 2703-2707.